

Stand-Off Distances on a Flat Flame Burner

COLIN R. FERGUSON

Department of Mechanical Engineering, Purdue University, West Lafayette, Indiana 47907

and

JAMES C. KECK

Department of Mechanical Engineering, Massachusetts Institute of Technology, Cambridge, Massachusetts 02139

For a given stand-off distance of a laminar flame on a porous metal burner, it has been shown both experimentally and theoretically that there exists two solutions, a low-speed flame and a high-speed flame. For small enough stand-off distance there is no solution. The minimum stand-off distance is identified as the quasi-steady approximation to the extinction length for flames quenching in flows perpendicular to a heat sink.

Measurements of flame speed, maximum flame temperature, and stand-off distance have been correlated for hydrogen, ethylene, and methane flames by a Peclet number dependent only on the ratio of the heat of combustion to the heat loss. The correlation agrees quantitatively with solution of one-dimensional flame equations where a Dirac-delta function models the reaction rate.

I. INTRODUCTION

This paper presents results of an experimental and theoretical study of non-adiabatic laminar flames [1]. It extends an earlier work [2] which predicted that for sufficiently large stand-off distances of a flame on a flat flame burner there would be both a high-temperature and a low-temperature solution. It was also predicted that there would be a minimum distance for which solutions exist. In the present work those predictions are experimentally verified and the earlier analysis is improved so that quantitative agreement is achieved between theory and experiment.

Both studies were motivated by and contribute to the practical problem of modeling the hydrocarbon and carbon monoxide emission from internal combustion engines. The analysis is

relevant to the problem of a transient flame propagating towards a wall and extinguishing at the quench distance. The minimum stand-off distance is a quasi-steady approximation to that quench distance. A complementary analysis of transient flame quenching has been made by Kurkov and Mirsky [3]. The quench distance computed by the quasi-steady model described later and their analysis is about the same. An important difference appears, however, in the amount of unburned fuel left at the wall after quenching has occurred, the quasi-steady model predicting nearly twice as much fuel in the quench layer.

The problem analyzed is a one-dimensional laminar flame with heat loss at the cold boundary. The energy and diffusion equations solved are those given by Spalding [4] with a Dirac-delta

function modeling the reaction rate. The analysis relates the flame speed, the burned gas temperature, and the stand-off distance. The experiments were designed to measure these three quantities.

II. THEORY

Assuming that all species have equal and constant specific heats at constant pressure, the energy equation for steady laminar flame propagation is taken to be [4]

$$\frac{d}{dx} \left[\lambda \frac{dT}{dx} \right] - \rho_u S_u c_p \frac{dT}{dx} + \rho_u S_u q \delta(D-x) = 0 \quad (1)$$

where the coordinate system is chosen so that the porous burner surface is at $x = 0$ and the flame is at $x = D$. The symbols in Eq. (1) are defined below:

λ	—thermal conductivity
T	—temperature
ρ	—density
S_u	—flame speed
q	—enthalpy of combustion per unit mass
$\delta(D-x)$	—Dirac-delta function with unity integral

Subscripts u and b refer to the unburned and burned states, respectively. The boundary conditions are:

$$\begin{aligned} T(0) &= T_u \\ T(\infty) &= T_b \quad \frac{dT}{dx}(\infty) = 0 \end{aligned} \quad (2)$$

In dimensionless variables the energy equation may be written as:

$$\frac{d^2\tau}{d\xi^2} - \frac{d\tau}{d\xi} + \delta(\text{Pe} - \xi) = 0 \quad (3)$$

where in terms of the adiabatic flame temperature $T_b^0 = T_u + q/c_p$

$$\tau = \frac{T - T_u}{T_b^0 - T_u}$$

$$\xi = \rho_u S_u c_p \int_0^x \frac{dx'}{\lambda}$$

$$\text{Pe} = \rho_u S_u c_p \int_0^D \frac{dx'}{\lambda}$$

The space variable ξ is a Peclet number based on distance x from the wall and Pe is the Peclet number based on the stand-off distance D . The boundary conditions are:

$$\begin{aligned} \tau(0) &= 0 \\ \tau(\infty) &= \tau_b \quad \frac{d\tau}{d\xi}(\infty) = 0 \end{aligned} \quad (4)$$

The solution to Eq. (3) subject to the boundary conditions (4) is

$$\tau = \begin{cases} \tau_b \left(\frac{\exp(\xi) - 1}{\exp(\text{Pe}) - 1} \right) & 0 < \xi < \text{Pe} \\ \tau_b & \xi \geq \text{Pe} \end{cases} \quad (5)$$

and the Peclet number based on stand-off distance is

$$\text{Pe} = \ln(1 - \tau_b)^{-1} = \ln \left(\frac{T_b^0 - T_u}{T_b^0 - T_b} \right) \quad (6)$$

A similar result has been derived by Kihara et al. [5] using an ignition temperature model.

The characteristic analysis for perpendicular flow presented previously (2) is, according to Eq. (6), strictly valid only for small Peclet numbers, in which case the left side may be integrated approximately and the right-hand side expanded into a Taylor series. The zero order approximation is

$$\text{Pe} \cong \frac{\rho_u S_u c_p D}{\lambda(D)} \cong \frac{T_b - T_u}{T_b^0 - T_b} \quad (7)$$

identical to that given in the previous paper.

The effect of chemical reactions on the stand-off distance given by Eq. (6) is entirely contained in the laminar flame speed, and since this can be measured experimentally, the inclusion of a

detailed chemical kinetic model is unnecessary. However, to check the sensitivity of the results to finite reaction rates, a more general analysis was carried out [1] in which the heat release rate was modeled by an overall Arrhenius rate equation. The results showed that Eq. (6) is a good approximation provided the $E/RT_b^0 \geq 7$, where E is a characteristic activation energy and R is the gas constant.

To proceed further, it is necessary to know the dependence of the flame speed on the flame temperature. Kaskan [6] has shown that the flame speed on porous metal burners often correlates empirically as

$$\frac{S_u}{S_u^0} = \exp \left[-\frac{E_A}{2R} \left(\frac{1}{T_b} - \frac{1}{T_b^0} \right) \right] \quad (8)$$

where S_u^0 is the adiabatic flame speed and E_A is an apparent activation energy. Combining Eqs. (6) and (8) yields a Peclet number based on the adiabatic flame speed and the stand-off distance

$$\begin{aligned} \text{Pe}^0 &= \rho_u S_u^0 c_p \int_0^D \frac{1}{\lambda} dx \\ &= \exp \left[\frac{E_A}{2R} \left(\frac{1}{T_b} - \frac{1}{T_b^0} \right) \right] \ln \left(\frac{T_b^0 - T_u}{T_b^0 - T_b} \right) \end{aligned} \quad (9)$$

Equation (9) can be used for computing stand-off distance given the adiabatic flame speed, the apparent activation energy, and the burned gas temperature. A typical solution of Eq. (9) is shown in Fig. 1. The Peclet number is a U-shaped function of temperature. It can be seen that for sufficiently large distances there is both a high-temperature and a low-temperature solution. There is also a minimum distance for which solutions exist.

The physical reason for this behavior is that for temperatures near the adiabatic flame temperature only a small amount of heat needs to be transferred to the burner to maintain a steady-state energy balance, hence the stand-off distance will be large. As the flame temperature decreases, the

heat loss per unit mass increases monotonically, so that the heat transfer to the burner must also increase and the standoff distance must decrease. However, at low enough temperatures, the energy generation decreases more rapidly with flame temperature than the heat loss per unit mass increases, so that the heat transfer to the burner must decrease and the stand-off distance must increase.

To compute the minimum stand-off distance, which is the quasi-steady approximation to the quench distance D_1 for the perpendicular flow, one must determine the temperature at which $\partial D/\partial T_b = 0$ so that by Eq. (9)

$$\frac{T_b}{\bar{\lambda}} \frac{\partial \bar{\lambda}}{\partial T_b} - \frac{E_A}{2RT_b} + \frac{T_b}{T_b^0 - T_b} \frac{1}{\ln \left(\frac{T_b^0 - T_b}{T_b^0 - T_u} \right)} = 0 \quad (10)$$

where

$$\frac{1}{\bar{\lambda}} = \int_0^D \frac{1}{\lambda} dx$$

The apparent activation energy of most flames is large enough that an asymptotic solution to Eq. (10) is adequate. The zero order equation for the burned temperature at quenching T_b^* is

$$\frac{T_b^0 - T_b^*}{T_b^0} \ln \left(\frac{T_b^0 - T_b^*}{T_b^0 - T_u} \right) \sim \frac{2RT_b^0}{E_A} \quad (11)$$

The solution of Eq. (11) is given in Fig. 2 for the special and most practical case $T_b^0 \gg T_u$. Comparison to an exact solution can be made with Fig. 1, which shows the Peclet number is minimum, for $E_A/2RT_b^0 = 5$, when $(T_b^0 - T_b)/T_b^0 = 0.072$. The corresponding value obtained from Fig. 2 is $(T_b^0 - T_b)/T_b^0 = 0.076$. Note that for large $E_A/2RT_b^0$ it takes very little heat to quench a flame so that temporal temperature changes during flame quenching are small and a quasi-steady approximation is valid.

Another parameter of interest in modeling hydrocarbon emission from internal combustion

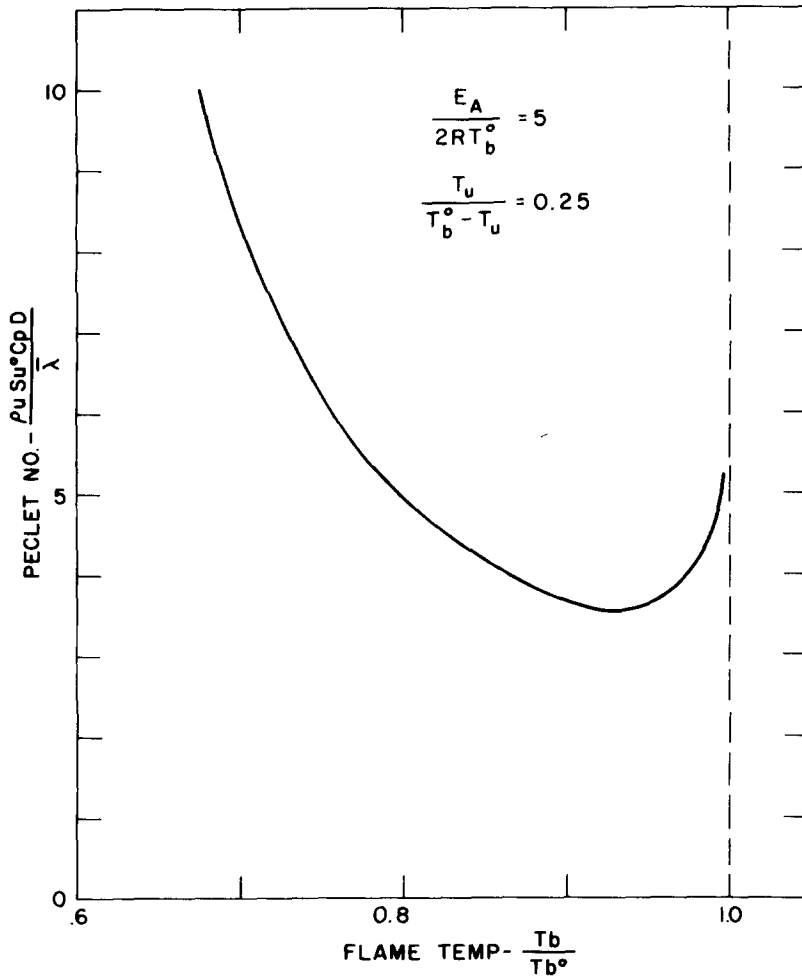


Fig. 1. Stand-off Peclet number based on adiabatic flame speed as a function of flame temperature.

engines is the mass of fuel left at the wall when the flame is quenched. To compute this parameter, a conservation equation for the fuel mass fraction C_A is introduced:

$$\frac{d}{dx} \left(\rho \mathcal{D} \frac{dC_A}{dx} \right) - \rho_u S_u \frac{dC_A}{dx} - \rho_u S_u \delta(D - x) = 0 \quad (12)$$

where \mathcal{D} is the diffusion coefficient for the fuel. Equation (12) can be derived when the binary diffusion coefficients of all pairs of species are equal or by postulating that all diffusion velocities obey Fick's law [7].

In dimensionless variables, Eq. (12) is:

$$\frac{1}{L} \frac{d^2 y}{d\xi^2} - \frac{dy}{d\xi} - \delta(\text{Pe} - \xi) = 0 \quad (13)$$

where $L = \lambda/\rho \mathcal{D} c_p$ is the Lewis number and $y = C_A/C_{A,u}$ is the normalized fuel mass fraction. The boundary conditions to impose on the fuel are:

$$y(\infty) = 0 \quad \frac{dy}{d\xi}(\infty) = 0 \quad (14)$$

and the solution is

$$y = 1 - \exp [L(\xi - \text{Pe})] \quad (15)$$

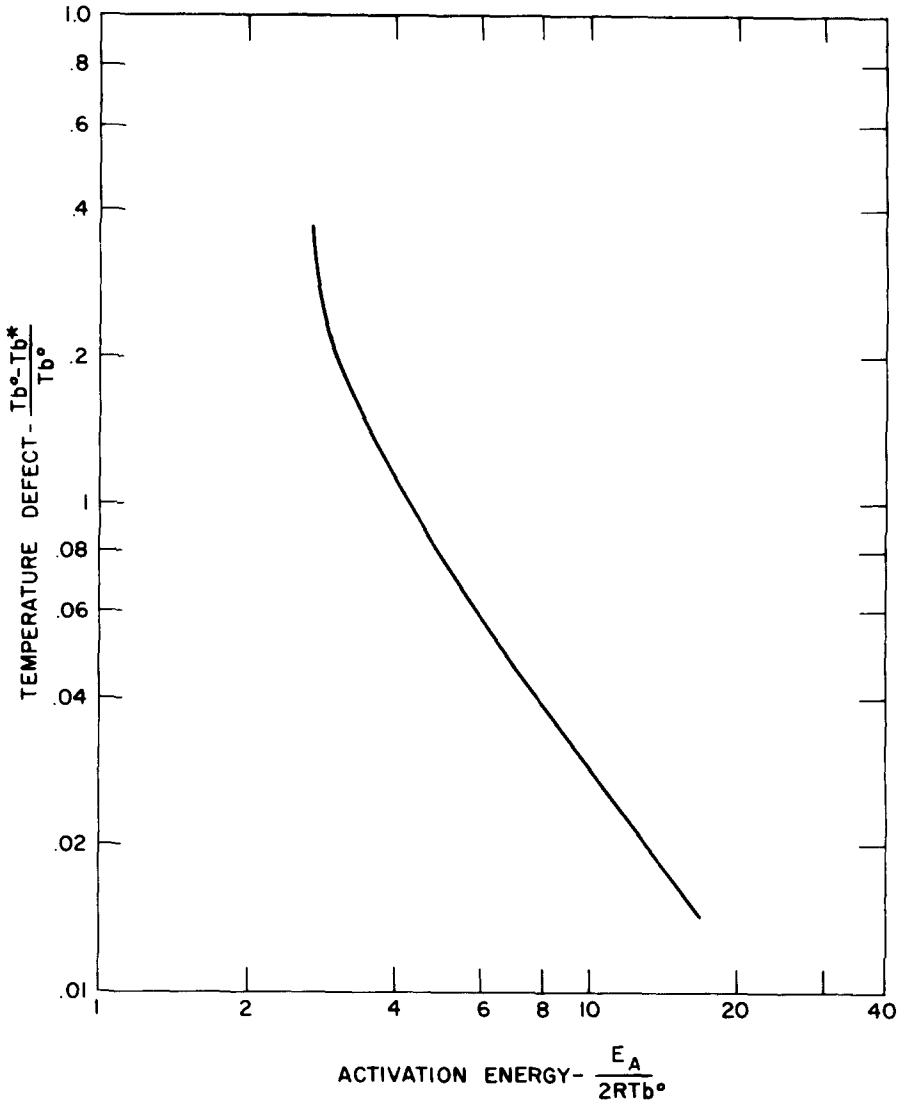


Fig. 2. Leading order asymptotic solution for the temperature at quenching.

Notice that $y(0) \neq 1$ and $(dy/d\xi)(0) \neq 0$; rather $y(0) - (1/L)(dy/d\xi)(0) = 1$, which shows that the reactant mass flux fraction at the burner exit plane is unity but that the composition is not pure reactants. Thus products are diffusing into the burner at the same rate that they are convected out. This is equivalent to the flame holder model of Hirschfelder et al. [8].

The mass of fuel per unit wall area, assuming $\rho\lambda = \rho_u\lambda_u$ is

$$\begin{aligned}
 m_q &= \int_0^D \rho C_A dx = \frac{C_{Au}\lambda_u}{S_u c_p} \\
 &\times \left(Pe - \frac{1}{L} [1 - \exp(-LPe)] \right) \\
 &= \rho_u C_{Au} D \frac{\lambda_u}{\lambda} \left(1 - \frac{1}{LPe} [1 - \exp(-LPe)] \right)
 \end{aligned}
 \tag{16}$$

The mass of fuel in a quench layer is computed by evaluating the Peclet number and flame speed, Eqs. (6) and (8), at the temperature of quenching T_b^* . Such calculations have been done under the conditions specified by Kurkov and Mirsky [3] for comparing their transient solution to the present quasi-steady model. When differences of definition are accounted for, good agreement is realized for the Peclet number but the quasi-steady model predicts about 1.75 times as much fuel as the quench layer.

III. EXPERIMENTS

The theoretical analysis relates the flame speed, the burned gas temperature, and the stand-off distance by a Peclet number dependent only on the ratio of the heat of combustion to the heat loss. The experiments were designed to check that relationship. The basic apparatus used to study the stand-off distance experimentally is a porous metal flat flame burner. The design is similar to Kaskan's [6] with three important differences. One, the 5.1-cm diameter burner sits atop a 15-cm diameter by 46-cm long plenum that creates a steady uniform velocity upstream of the porous metal. Two, the cooling coils were located in the middle of the porous plug, seven diameters from the exit plane of the burner, in order to minimize velocity nonuniformities at the exit plane. The velocity of gas issuing from the burner in the absence of combustion was measured with a hot-wire anemometer and found to be uniform over the burner surface to within $\pm 5\%$. The third difference was the inclusion of an outer annulus of porous metal through which nitrogen flowed. This served to eliminate entrainment of air by the burned gases downstream of the flame and improved the flame stability for low-velocity flames, so that a stabilizing screen in the burned gases was not necessary.

The temperature of the exit plane of the burner was measured by two 250- μ iron-constantan thermocouples in 1.6-mm diameter protective sheaths imbedded in the porous metal 1 mm from the surface. One was located at the center and the other at the edge of the burner. The burner temperature was controlled by varying

either (or both) the temperature of the cooling water or of the nitrogen. The two thermocouple temperatures differed by less than 30 K. This is an important advantage of Kaskan's design over the edge cooled burner discussed by Kihara et al. [5].

The flow rates of fuel and air were controlled by critical flow orifices calibrated by either a mercury-sealed piston displacement meter or a liquid displacement technique. The reactants were premixed in a mixing chamber upstream of the plenum.

Flame temperatures were measured by monitoring the radiation emitted from a fine wire held in the flame, a technique called hot-wire pyrometry [9]. The hot-wire pyrometer and the burner are shown in Fig. 3. A 25-micron Pt-13 percent Rh wire was held in tension parallel to the burner surface by the spring loaded probe shown in the figure. This was the smallest wire that could be held in tension and survive in the flame for many hours. A thermocouple was not used, because the welded junction of fine wire thermocouples is twice the wire diameter; hence spatial resolution would have been reduced by a factor of two. The wire was coated with a film of quartz by immersion into the hot gases from a flame in which a small amount of hexamethyldisiloxane had been burned [6]. The diameter of the wire after coating was measured under a microscope and typically was 35 μ . The purpose of the coating is to kill catalytic heating of the wire.

An image of a 3-mm long section of the wire was focused by a cylindrical lens on the entrance slit of a photomultiplier. The image on the cathode is diffuse and covers the whole photosensitive area. An orange filter was used to minimize flame radiation seen by the photomultiplier. With an electrically heated wire it was determined that the overall sensitivity of the hot-wire pyrometer varied less than 2% over a wire translation of 5 mm.

The photomultiplier signal V depends on wire temperature T_w to a power like 14. The calibration curve is given by:

$$V = AT_w^{7/4} \exp(-BT_w^{-1/2}) \quad (17)$$

where A and B are the calibration constants that are discussed in reference [9]. Because the wire is

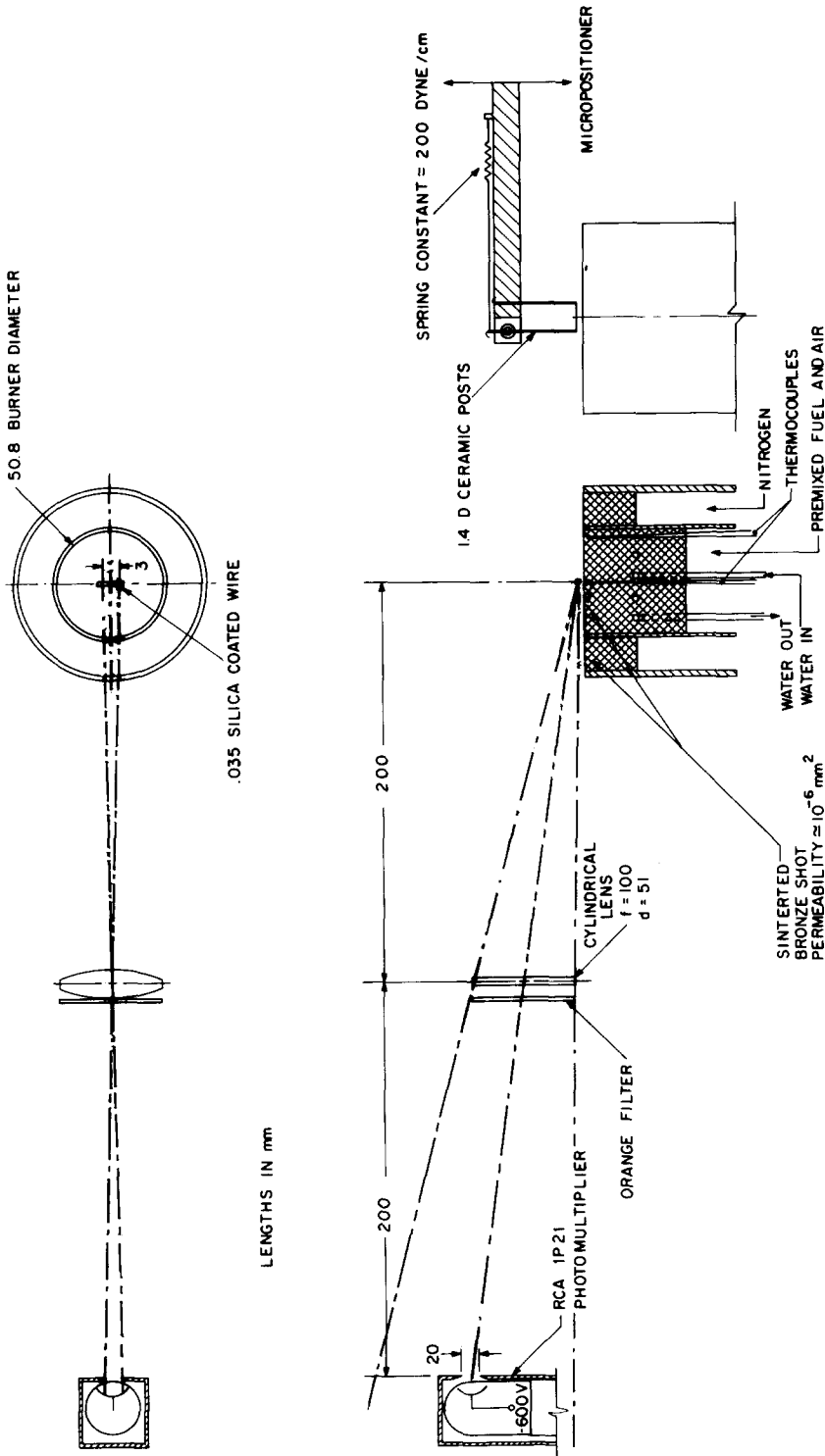


Fig. 3. Experimental apparatus; flat flame burner and hot-wire pyrometer.

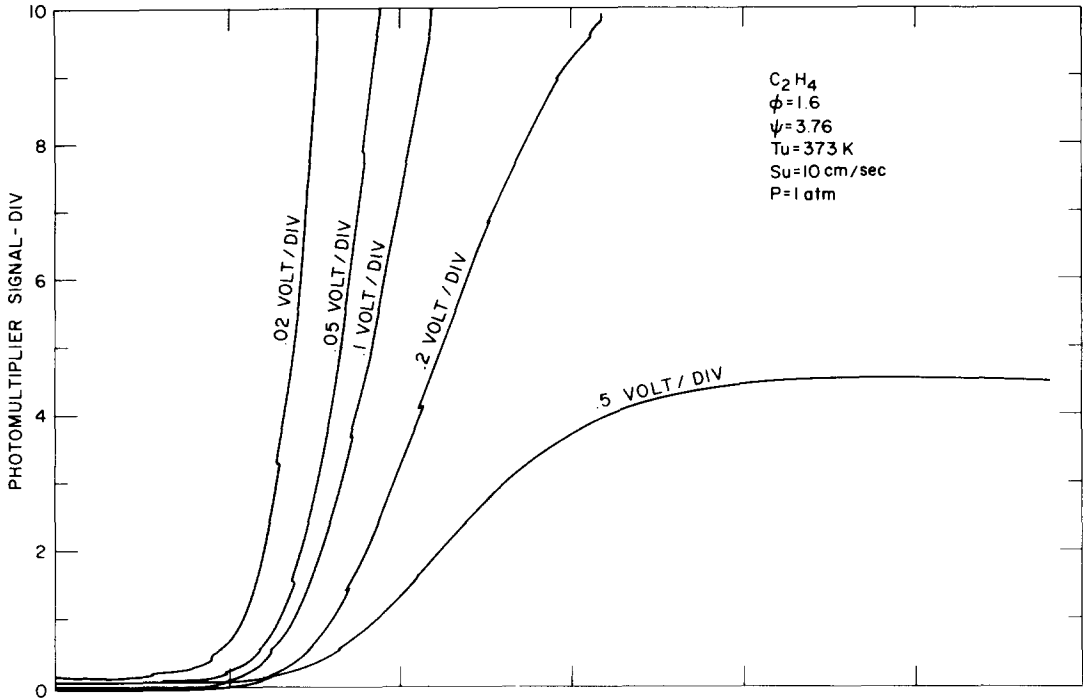


Fig. 4(a) Intensity signal versus distance for ethylene-air flame. ϕ is the fuel-air equivalence ratio, and ψ is the molar nitrogen to oxygen ratio of the reactants.

radiating, its temperature is slightly less than the gas temperature. To estimate heat transfer to the wire the following correlation of Nusselt number N_u and Peclet number P_0 based on wire diameter was used [10]:

$$N_u \sim \frac{2}{\ln\left(\frac{4.492}{P_0}\right)} \quad (P_0 \rightarrow 0) \quad (18)$$

This gives a radiation correction to the burned gas temperature:

$$T_b - T_w = \frac{\epsilon \sigma T_w^4 d}{2\lambda_b} \ln\left(\frac{4.492\lambda_b}{\rho_u S_u c_p b d}\right) \quad (19)$$

where ϵ is wire emissivity, σ is the Stefan-Boltzmann constant, and d is the wire diameter. The emissivity of the coated wire is $\epsilon = 0.22$ (6). The equilibrium burned thermal conductivity and

specific heat were calculated by the computer program of Svehla and McBride [11] at the wire temperature. These corrections were typically 50 K.

The temperature profile in the flame was measured by moving the cantilever probe down to the burner surface. The ceramic posts of the probe were designed to slip when contact occurred with the burner surface. Screwing the micropositioner down until the posts slip establishes the zero coordinate. The wire is then moved away from the burner and an x - y recorder slaved to the micropositioner plots the photomultiplier signal versus wire position. The measurement is usually repeated at four different sensitivities on the x - y recorder, in order to locate the inflection point of the temperature profile (the stand-off distance) with precision. The repeated measurements also serve to establish an average reading for the zero coordinate. To account for the probe's influence on the apparent flame position, five wire diameters have been added to the distance measurements [12].

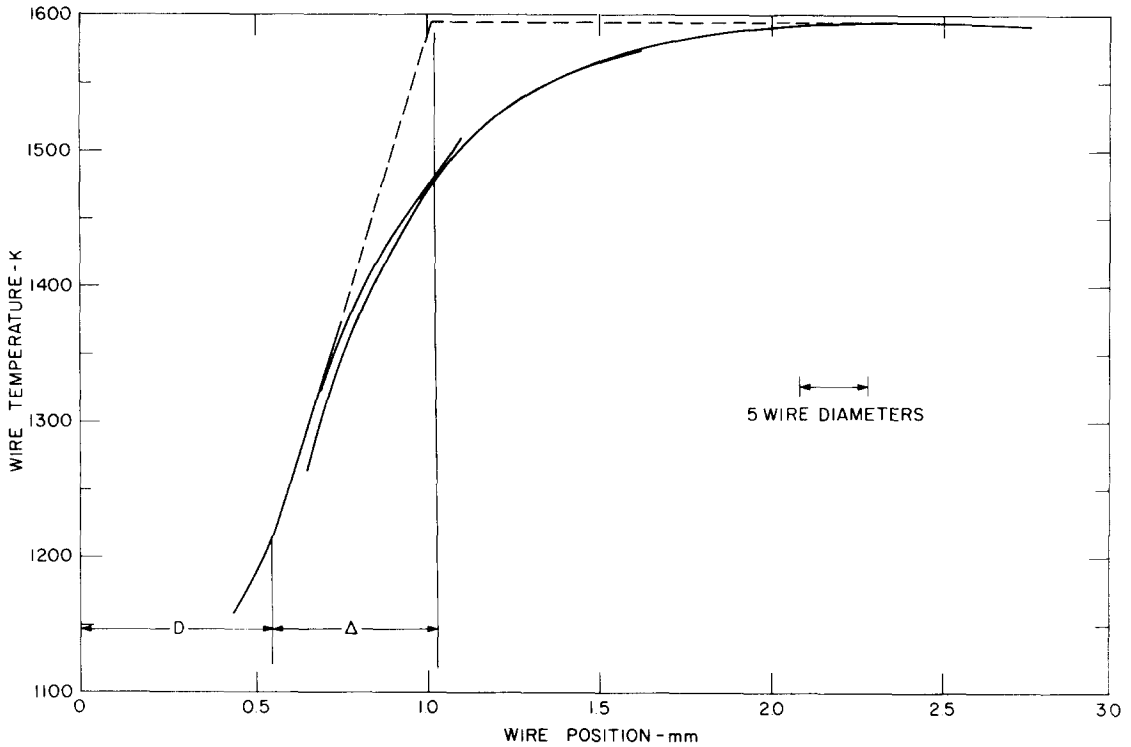


Fig. 4(b) Wire temperature versus distance for the same. The reaction zone thickness is $\Delta = (T_b - T_i)/(dT/dx)_i$; where i denotes the inflection point.

The inflection point of the temperature profile was chosen to define the stand-off distance instead of the maximum because the maximum occurs in a region of slowly varying temperature, so that its position is determined in part by the radiative losses from the burned gases and in part by the small variations in detector sensitivity with wire position.

An intensity distance diagram is shown in Fig. 4 together with the wire temperature distance plot. It is clear from these curves that the zero coordinate is accurate only to ± 0.1 mm. Note that the reaction zone thickness is not small compared to the stand-off distance. Even modeling the heat release by an overall Arrhenius rate equation does not admit this possibility [1]. The problem is that there are many reactions characterizing the heat release. In a hydrocarbon flame, one-half to two-thirds of the heat release is associated with the formation of CO and H₂O in a zone labeled the primary reaction zone by Fristrom and Westen-

berg [12]. There is a secondary reaction zone where CO burns up, recombination takes place, and the remaining heat is released. In a hydrogen flame, one expects most of the heat release to be by three-body recombination reactions, so what was the secondary reaction zone in a hydrocarbon flame is the primary zone of heat release in a hydrogen flame. These considerations are not important for computing stand-off distance, since the experimental results that follow indicate that most of the heat release of all these flames is fast enough to be characterized by a single temperature T_b .

Two sets of experiments were performed: one at constant equivalence ratio and one at constant flame speed. For each flame, the wall temperature was held constant. Because the cooling coils were 22 mm below the exit plane of the burner, the surface temperature was a strong function of conditions and could be varied by only ± 25 K. The conditions studied were chosen to keep that

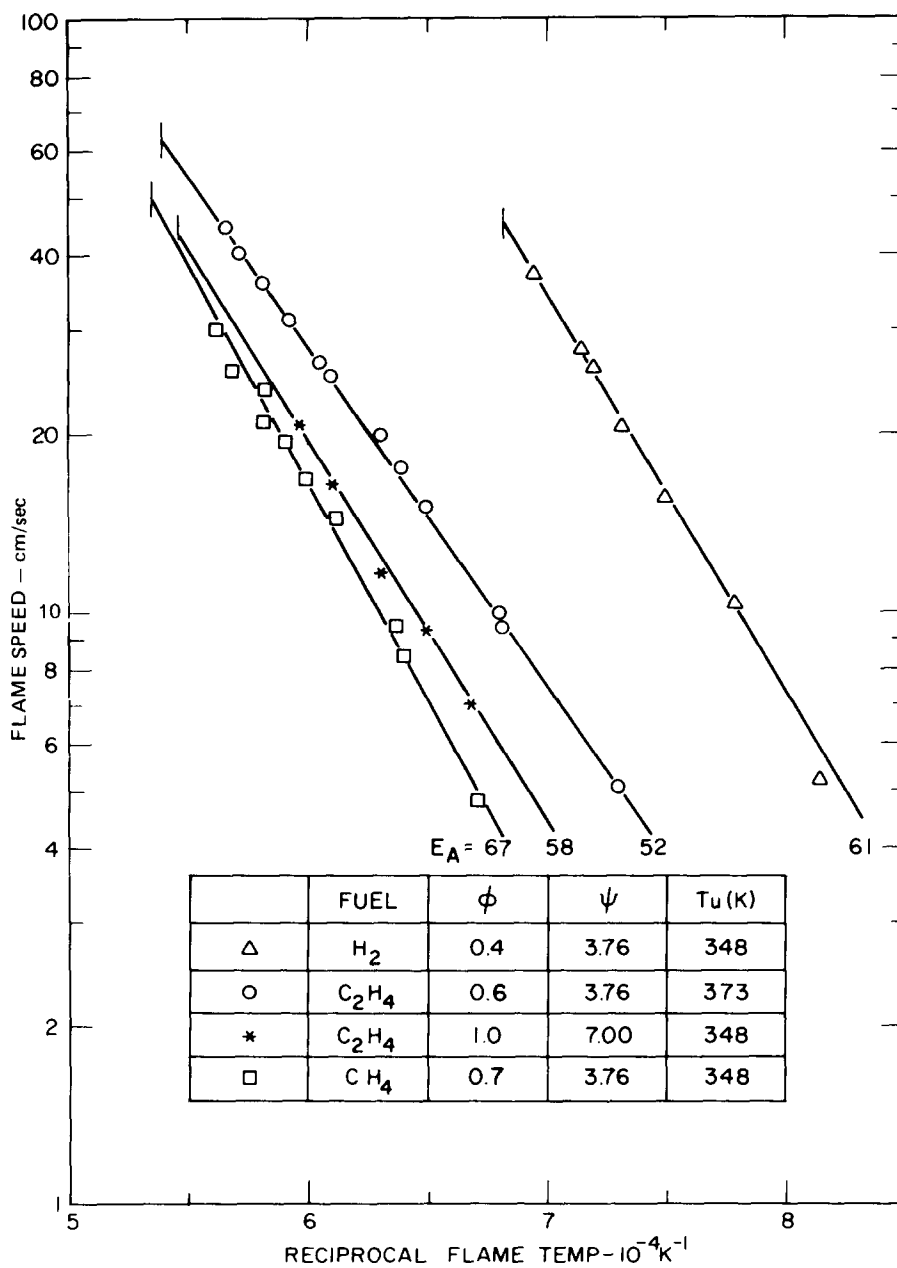


Fig. 5. The dependence of flame temperature on burning velocity. The apparent activation energies in kcal/mole are given at the bottom of each curve; they agree with Kaskan's [6] within $\pm 18\%$.

temperature constant so that only one parameter was varied at a time. A better burner would use smaller cooling coils.

The data at constant equivalence ratio are given in Figs. 5 and 6. In agreement with theoretical

prediction, it was found that for a given stand-off distance based on the inflection point in the temperature profile there is indeed both a high-temperature and a low-temperature solution. These results should not be confused with Spalding's

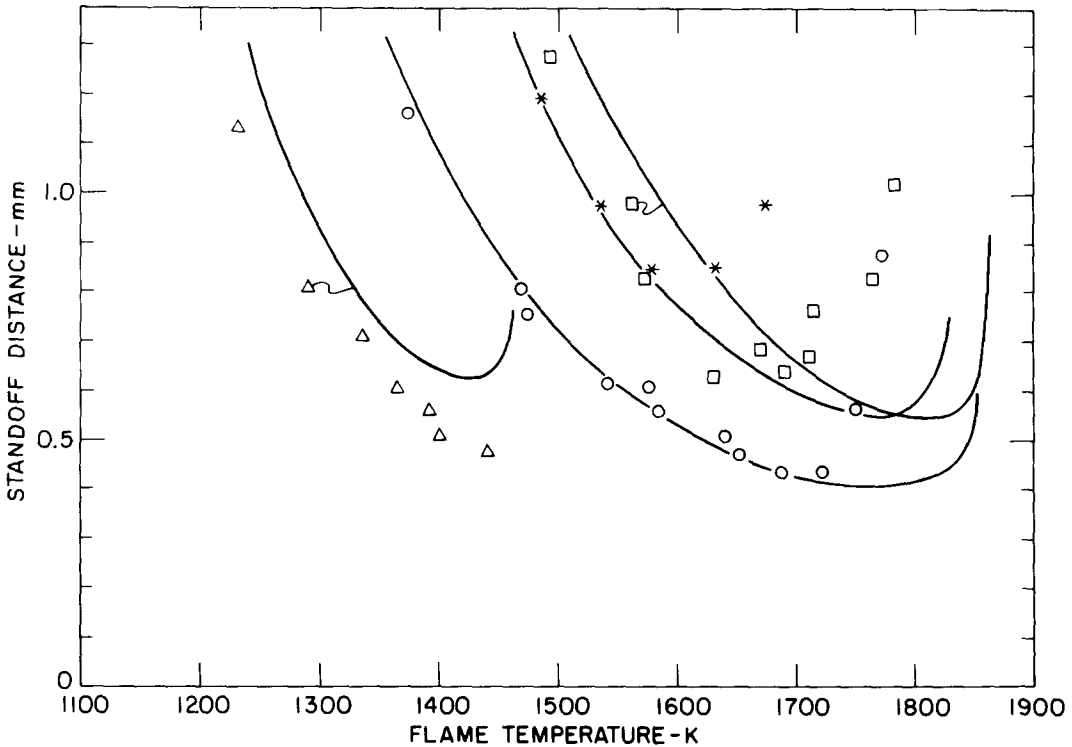


Fig. 6. The dependence of stand-off distance on flame temperature. The data key is given in Fig. 5. The solid curves are the theoretical function given in Eq. (9).

prediction [13] that in the presence of distributed heat loss and heat release there are two solutions for a given heat loss per unit mass (i.e. flame temperature); rather there is a high-temperature and a low-temperature solution for a given heat loss to the burner.

Similar to other reports [6, 14, 15], instabilities and three-dimensional phenomena have been observed. For flame speeds comparable to velocity fluctuations in the room, a flickering flame was observed. A further reduction in speed caused extinguishment.

For hydrocarbon-air flames a corrugated or wrinkled flame appeared for temperatures slightly larger than T_b^* . If the flow rate is increased further the temperature becomes independent of flame speed, and eventually the flame is blown off. The wrinkling mechanism can be explained by arguing that the stand-off distance-temperature relationship illustrated by Fig. 1 is valid for any streamtube. It can be seen that for nearly adiabatic flames, the small velocity (flame temperature)

variations from streamtube to streamtube cause large variations in local stand-off distance.

The hydrogen used in these experiments had enough hydrocarbon impurities so that in a dark room the flame was luminous. It appears that the high-temperature solution for this flame is unstable, since a cellular structure was observed for temperatures greater than the temperature T_b^* of minimum stand-off distance. The maximum temperature of these flames increased monotonically (although not linearly on the Arrhenius plot) with flame speed up to the highest speed measured, about twice the apparent adiabatic flame speed. The appearance of cellular flames indicates the occurrence of selective diffusion. Since these cells are three dimensional, temperatures larger than the equilibrium adiabatic flame temperature could be explained by shifts of composition due to selective diffusion.

The hydrogen-air flames also showed anomalous behavior regarding catalytic heating of the wire. For bare wires, unlike hydrocarbon flames

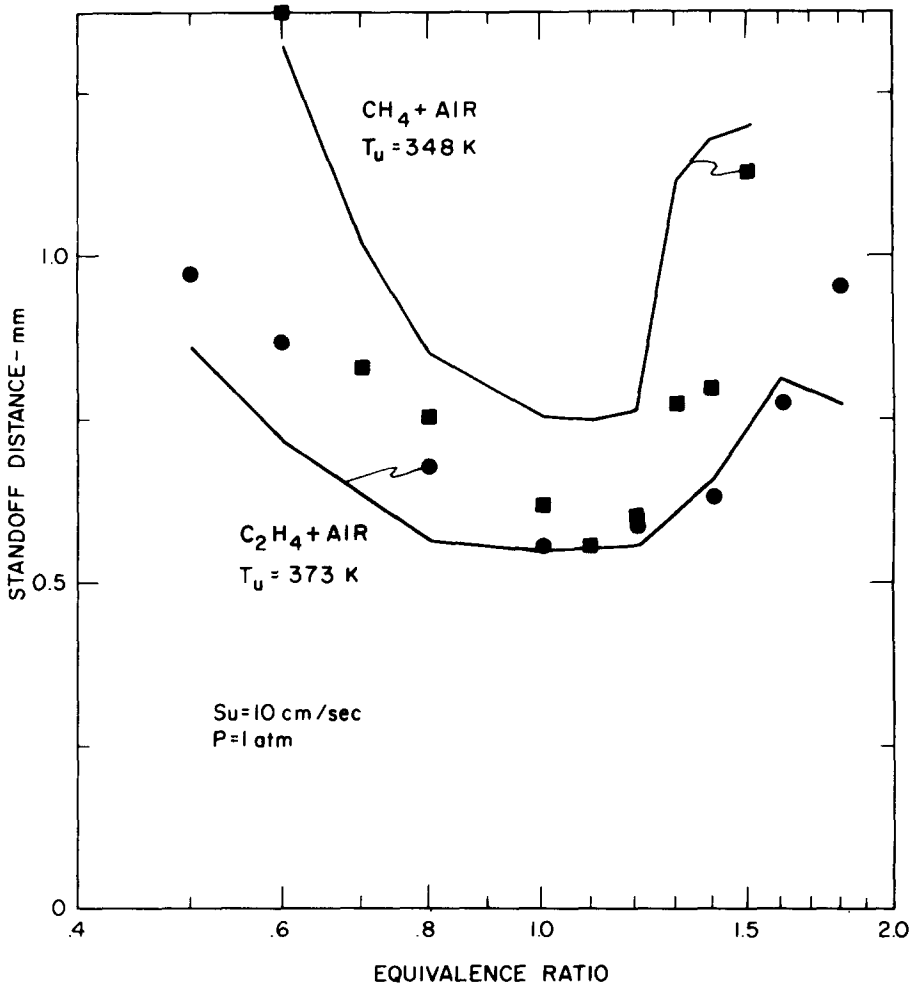


Fig. 7. The dependence of stand-off distance on equivalence ratio. The solid curves are the theoretical function given in Eq. (6); they are kinky because measured T_b have been used.

where only one maximum of wire temperature is observed, there were two, the largest of which occurs is the preheat zone.

The stand-off distance as a function of equivalence ratio at constant flame speed is given in Fig. 7. The stand-off distance as a function of equivalence ratio has a minimum near $\phi = 1$, because the heat released in the reaction zone is a maximum at this point. The stand-off distance is determined by a balance of conduction and convection, and since the flame speed is held constant the stand-off distance must get smaller as the heat released increases.

The lean limit at these speeds appears deter-

mined by the onset of Taylor instabilities in the burned gases which are characterized by the formation of holes in the flame [14]. The rich limit for methane was caused by flow-off, whereas for ethylene measurements at $\phi > 1.8$ could not be made because radiating soot particles masked the wire. Another instability appeared for the methane-air flame. At equivalence ratios of $\phi = 1.2, 1.3,$ and 1.4 , surface waves travelled along the flame causing pressure fluctuations that were audible. The disturbances were small enough, however, that the mean stand-off distance has been presented in the figures.

According to the theory for all flames with a

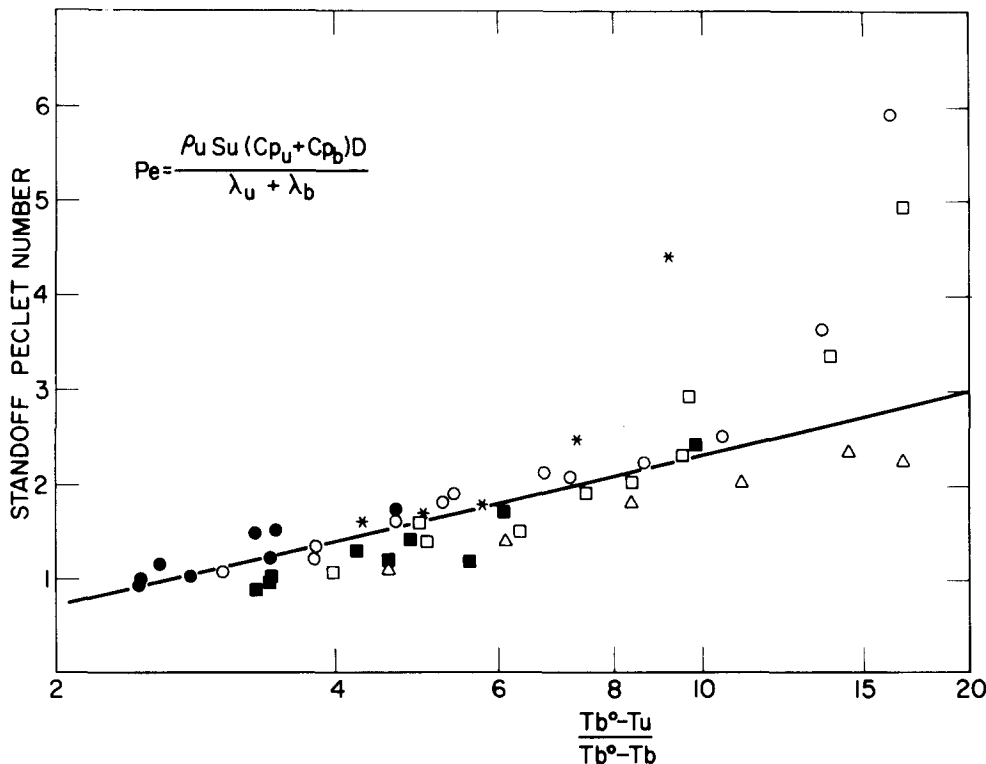


Fig. 8. Stand-off Peclet number as a function of the ratio of the heat of combustion to the heat loss. The line is the theoretical curve given as Eq. (6). The data key is given in Figs. 6 and 7.

dimensionless activation energy E/RT_b^0 greater than about 7, there should be a universal plot of Peclet number versus the ratio of the heat of combustion to the heat loss. To test the theory an experimental Peclet number has been defined as:

$$Pe = \frac{\rho_u S_u (c_{pu} + c_{pb}) D}{\lambda_u + \lambda_b} \quad (20)$$

where the thermochemical and transport data needed for the definition have been computed using the program of Svehla and McBride [11].

Figure 8 shows quantitative agreement between the theoretical Peclet number and the experimental data. Indeed the gross behavior of the flames studied is described by a single curve which is the logarithm of the ratio of heat of combustion to the heat loss. The measurements are not accurate enough to study the small deviations that may be due to the finite heat release zone. It is clear that the heat flux at the wall normalized by the

temperature rise, the stand-off distance, and the thermal conductivity of the burned gases is not a constant as assumed previously [1].

For values of $(T_b^0 - T_u)/(T_b^0 - T_b)$ greater than about 10 there are large deviations from the plot caused by the smallness of the quantity $T_b^0 - T_b$. These errors are just large enough that they cannot be dismissed as only experimental uncertainty. Rather it appears that hydrocarbon flames do not burn to thermodynamic equilibrium. For example, any carbon monoxide in the products that is neglected in computing the adiabatic flame temperatures causes T_b^0 , hence $T_b^0 - T_b$, to be overpredicted.

Finally, the correlation works for the hydrogen-air flame despite the fact that the specific heat and diffusivity of hydrogen are an order of magnitude larger than those of the other stable species in the flame. The theory is adequate because there is so much nitrogen in the flame that very little of the sensible enthalpy is tied up in the hydrogen. The

assumption that all species in the flame have equal specific heats and diffusivities is not expected to be valid in a hydrogen-oxygen flame.

IV. CONCLUSIONS

1. The Peclet number based on stand-off distance depends only on the ratio of the heat combustion to the heat loss provided that (1) the dimensionless activation energy $\beta = E/RT_b$ is greater than about 7 and (2) that when hydrogen is a reactant it carries little of the sensible enthalpy.

2. There is a minimum stand-off distance that, because so little heat is required to quench a flame, is a good approximation to the quench distance for an unsteady flow.

3. An expression has been derived for the fuel per unit area in a quench layer. It needs to be checked experimentally because the diffusion of products into a flat flame burner has never been observed.

The authors are grateful to the General Motors Corporation for funding this work.

REFERENCES

1. Ferguson, C. R., Stand-off Distances on a Flat Flame Burner, Ph.D. Thesis, Dept. Mech. Eng., M.I.T., Cambridge, Mass., Sept. 1977.

2. Ferguson, C. R., and Keck, J. C., *Combust. Flame* 28:197-205 (1977).
3. Kurkov, A. P., and Mirsky, W., *Twelfth Symposium (Int.) on Combustion*, The Combustion Institute, Pittsburgh, 1969, p. 615.
4. Spalding, D. B., *Combust. Flame* 1:296-307 (1957).
5. Kihara, D. H., Fox, J. S., and Kinoshita, C. M., *Combust. Sci. Technol.* 11:239-246 (1975).
6. Kaskan, W. T., *Sixth Symposium (Int.) on Combustion*, Williams and Wilkins, Baltimore, 1953 p. 126.
7. Williams, F. A., *Combustion Theory*, Addison-Wesley, Reading, Mass., 1965, p. 11.
8. Hirschfelder, J. O., Curtiss, C. F., and Bird, R. B., *Molecular Theory of Gases and Liquids*, John Wiley & Sons, Inc., New York, 1954, p. 761.
9. Ferguson, C. R., and Keck, J. C., Hot-Wire Pyrometry, *J. Appl. Phys.* 49:3031-3032 (1978).
10. Illingworth, C. R., *Laminar Boundary Layers* (L. Rosenhead, ed.), Oxford University Press, Oxford, England, 1963, p. 163.
11. Svehla, R. A., and McBride, B. J., NASA TN D-7056 (1973).
12. Fristrom, R. M., and Westenberg, A. A., *Flame Structure*, McGraw-Hill, New York, 1965, p. 251 and 305.
13. Spalding, D. B., *Combust. Flame* 1:296-307 (1957).
14. Kydd, P. H., and Foss, W. I., *Combust. Flame* 8: 267-273 (1964).
15. Botha, J. P., and Spalding, D. B., *Proc. Royal Soc. Ser. A* 225:71-96 (1954).

Received 17 February 1978; revised 16 May 1978